0026-895X/06/6904-1166–1173
MOLECULAR PHARMACOLOGY
U.S. Government work not protected by U.S. copyright
Mol Pharmacol 69:1166–1173, 2006

Vol. 69, No. 4
19158/3099339
Printed in U.S.A.

Kinetics of Penetration Influence the Apparent Potency of Vanilloids on TRPV1

Jozsef Lazar, Derek C. Braun, Attila Tóth,[1] Yun Wang,[2] Larry V. Pearce, Vladimir A. Pavlyukovets, Peter M. Blumberg, Susan H. Garfield, Stephen Wincovitch, Hyun-Kyung Choi, and Jeewoo Lee

Laboratory of Cellular Carcinogenesis and Tumor Promotion (J.L., D.C.B., A.T., Y.W., L.V.P., V.A.P., P.M.B.) and Laboratory of Experimental Carcinogenesis (S.H.G., S.W.) National Cancer Institute, National Institutes of Health, Bethesda, Maryland; Department of Biology, Gallaudet University, Washington DC (D.C.B.); and Research Institute of Pharmaceutical Sciences, College of Pharmacy, Seoul National University, Seoul, South Korea (H.-K.C., J.L.)

Received September 21, 2005; accepted January 13, 2006

ABSTRACT

Evidence that the ligand binding site of TRPV1 lies on the inner face of the plasma membrane and that much of the TRPV1 itself is localized to internal membranes suggests that the rate of ligand entry into the cell may be an important determinant of the kinetics of ligand action. In this study, we synthesized a BODIPY TR-labeled fluorescent capsaicin analog (CHK-884) so that we could directly measure ligand entry. We report that CHK-884 penetrated only slowly into Chinese hamster ovary (CHO) cells expressing rat TRPV1, with a $t_{1/2}$ of 30 $\pm$ 4 min, and localized in the endoplasmic reticulum and Golgi. Although CHK-884 was only weakly potent for TRPV1 binding (K_i = 6400 $\pm$ 230 nM), it was appreciably more potent when assayed by intracellular calcium imaging and was 3.2-fold more potent with a 1-h incubation time (37 nM) than with a 5-min incubation time. Olvanil, a highly lipophilic vanilloid, yielded an EC_{50} of 4.3 nM upon intracellular calcium imaging with an incubation time of 1 h, compared with an EC_{50} value of 29.5 nM for calcium imaging assayed at 5 min. Likewise, the antagonist 5-iodo-resiniferatoxin (5-iodo-RTX) displayed a K_i of 4.2 pM if incubated with CHO-TRPV1 cells for 2 h before addition of capsaicin compared with 1.5 nM if added simultaneously. We conclude that some vanilloids may have slow kinetics of uptake; this slow uptake may affect assessment of structure activity relations and may represent a significant factor for vanilloid drug design.

TRPV1 is a central nociceptor mediating response to vanilloids (such as capsaicin and RTX), heat, low pH, and endogenous ligands (Szallasi and Blumberg, 1989; Caterina et al., 1997; Zygmunt et al., 1999; Hwang et al., 2000; Gavva et al., 2004). In addition, it has a prominent role in the functioning of C-fiber sensory neurons, thus becoming a promising therapeutic target for chronic pain, bladder hyperreflexia, pruritus, diabetic neuropathy, postherpetic neuropathy, or cough (Robbins, 2000; Morice and Geppetti, 2004).

In this study, we were concerned with the influence of the rate of vanilloid penetration into the cell on apparent vanilloid activity. It is clear that TRPV1 shows complicated cellular localization. Contrary to the expectation that TRPV1 should be localized at the plasma membrane, most seems to be located at internal membranes (Olah et al., 2001). Consistent with this pattern of localization, multiple research groups have shown that TRPV1 can function to release calcium from endoplasmic stores as well as permit calcium entry from outside the cell (Eun et al., 2001; Marshall et al., 2003). Vanilloids obviously need to penetrate into the cell to gain access to the endoplasmic reticulum localized TRPV1.

For the TRPV1 located at the plasma membrane, the original view was, likewise, that the vanilloid binding site of

This research was supported in part by the Intramural Research Program of the National Institutes of Health, National Cancer Institute, Center for Cancer Research and by grants from the Basic Research Program of the Korea Science and Engineering Foundation (RO1-2004-000-10132-0).

[1] Current affiliation: University of Debrecen, Department of Cardiology, Debrecen, Hungary.

[2] Current affiliation: Neuroscience Research Institute, Peking University, Beijing, China.

Article, publication date, and citation information can be found at http://molpharm.aspetjournals.org.
doi:10.1124/mol.105.019158.

ABBREVIATIONS: TRPV, transient receptor potential vanilloid-related; rTRPV1, cloned rat vanilloid receptor subtype 1; CHO-rTRPV1, rat vanilloid receptor expressing CHO cells; rTRPV1-GFP, green fluorescent protein labeled rat TRPV1; I-RTX, 5-iodo-resiniferatoxin.; RTX, resiniferatoxin; DPBS, Dulbecco's phosphate-buffered saline; BSA, bovine serum albumin; RTX, resiniferatoxin; CHO, Chinese hamster ovary; $[Ca^{2+}]_i$, intracellular Ca^{2+}; CHK-884, *N*-(BODIPY TR cadaverine)-2-(4-hydroxy-3-methoxyphenyl)acetamide or *N*-{5-[({4-[4,4-difluoro-5-(2-thienyl)-4-bora-3*a*,4*a*-diaza-*s*-indacene-3-yl]phenoxy}acetyl)amino]pentylamino}-2-(4-hydroxy-3-methoxyphenyl)acetamide; GFP, green fluorescent protein.

TRPV1 lies on the inner face of the plasma membrane. Oh and coworkers reported that DA-5018, a capsaicin derivative bearing a primary amine, activated single channel currents only when applied to the inner surface of the membrane and not when applied to the outer surface (Jung et al., 1999). Mutational studies have identified residues on the third and fourth transmembrane domains of TRPV1 as being important determinants of ligand binding, arguing that this is indeed the site of ligand binding (Jordt and Julius, 2002; Chou et al., 2004; Gavva et al., 2004; Phillips et al., 2004). Furthermore, activity of anandamide on TRPV1 depends on its uptake by a transport system (De Petrocellis et al., 2001). On the other hand, Rami et al. (2004) have reported that a TRPV1 antagonist that contained a quaternary amine was effective only when applied to the external surface of membranes in patch clamp studies, and Vyklicky et al. (2003) reported that intracellular application of vanilloids was insufficient for activating TRPV1 channels in human embryonic kidney 293T cells. It thus remains uncertain whether vanilloids must enter the cell to regulate that portion of TRPV1 localized at the plasma membrane.

In this article, we describe the synthesis of a fluorescent vanilloid. We measured its rate of uptake into cells directly, we showed that this uptake was slow, and we demonstrated that at limiting doses the compound only slowly elevated intracellular calcium levels. We further describe that the biological potencies of the agonist olvanil and the antagonist 5-iodo-RTX showed marked time dependence, presumably reflecting their slow penetration into cells. We have reported previously that the lipophilic vanilloid homovanilloyl-hexadecylamide only slowly equilibrated with TRPV1 in membrane preparations (Szallasi et al., 1991). An important implication of our findings for vanilloid structure activity analysis is that short incubation times may substantially underestimate potencies for some structural series of vanilloids.

Materials and Methods

Synthetic Procedure and Spectra of CHK-884. A solution of BODIPY (5 mg, 0.01 mmol; Invitrogen, Carlsbad, CA) and pentafluorophenyl (4-hydroxy-3-methoxyphenyl)acetate (4 mg, 0.01 mmol) in CH_2Cl_2 (1 ml) was treated with triethylamine (1 drop) and stirred for 2 h at the room temperature. The reaction mixture was concentrated in vacuo and the residue was purified by preparative TLC (silica gel) using CH_2Cl_2:MeOH (5:1) as eluant to afford CHK-884 as a purple solid (4 mg, 67%). ^{1}H NMR ($CDCl_3$, 500 MHz) δ6.65–8.1 (m, 15 H, Ar), 6.56 (bt, 1 H, NH), 5.47 (bt, 1 H, NH), 4.55 (s, 2 H, OCH_2CONH), 3.87 (s, 3 H, OCH_3), 3.45 (s, 2 H, $OCCH_2Ar$), 3.33 (dd, 2 H, CH_2NH), 3.18 (dd, 2 H, CH_2NH), 1.54 (m, 2 H, CH_2), 1.45 (m, 2 H, CH_2), 1.28 (m, 2 H, CH_2); MS (FAB) 695 $[M+Na]^+$; high resolution mass spectrometry (fast atom bombardment) *m/z* calculated for $C_{35}H_{35}BF_2N_4O_5S$ $[M+H]^+$ 673.2389, found 673.2446.

Cell Culture and Transfection. The CHO-rTRPV1 cell line (Tet-Off system) was a generous gift of James E. Krause and Daniel N. Cortright (Neurogen Corp., Branford, CT). Cells were maintained in Ham's F12 medium with 1 mM L-glutamine supplemented with 10% fetal bovine serum, 25 mM HEPES buffer, pH 7.2, 250 μg/ml G418 (Geneticin) (all from Invitrogen), and 1 μg/ml tetracycline (Calbiochem, La Jolla, CA). To induce TRPV1 expression, maintaining medium was replaced with inducing medium (maintaining medium without G418 and tetracycline). Where indicated, CHO cells used for confocal microscopy were cultured in F-12K medium with 2 mM L-glutamine and 10% FBS and were transfected with Lipofectamine 2000 following the manufacturer's directions using 2 μg of a plasmid encoding rTRPV1-GFP fusion protein (Olah et al., 2001).

[^{3}H]RTX Binding Assay. Binding assays were carried out in Dulbecco's phosphate-buffered saline (DPBS; Invitrogen) containing 0.25 mg/ml bovine serum albumin (BSA; Sigma, St. Louis, MO). 100 μl of CHO-rTRPV1 cell pellet (which corresponds to 1/15 of the contents of a T75 flask of confluent, induced CHO-rTRPV1 cells) was incubated in a 350-μl final volume with different concentrations of the competing ligand and 100 pM [20-^{3}H]resiniferatoxin ([^{3}H]RTX; PerkinElmer Life and Analytical Sciences, Boston, MA) at 37°C. Nonspecific binding was measured in the presence of 100 nM nonradioactive RTX (Alexis, San Diego, CA). After 60 min, the mixture was cooled on ice; nonspecific binding of [^{3}H]RTX was reduced by addition of 200 μg/tube bovine glycoprotein fraction VI (AGP; MP Pharmaceuticals, Irvine, CA). After 15-min incubation on ice, the whole mixture was transferred to 1.5-ml plastic, capped centrifuge tubes and centrifuged in a benchtop centrifuge (15 min, 12,200 rpm, 4°C; Allegra 21R; Beckman Coulter, Fullerton, CA). To determine the concentration of free [^{3}H]RTX, 200-μl aliquots of supernatant were transferred to scintillation vials. Membrane bound [^{3}H]RTX was determined from the pellets. K_i values were calculated using Origin software (OriginLab Corp., Northampton, MA).

^{45}Ca Uptake Measurement. rTRPV1 expressing CHO cells were plated in maintaining medium onto 24-well plates at 20 to 40% confluence. The next day, the medium was removed, cells were washed twice with DPBS, and the medium was replaced with inducing medium. ^{45}Ca uptake measurements were performed 48 h after the change to inducing medium, when the cells were almost confluent. For measurement of ^{45}Ca uptake, plates were incubated for 5 min at 37°C in a water bath in 400 μl of Dulbecco's modified Eagle's medium (Invitrogen) containing 1.8 mM $CaCl_2$, 0.25 mg/ml BSA (unless otherwise stated), 1 μCi of $^{45}Ca^{2+}$ (MP Pharmaceuticals) and the different concentrations of the compound being tested. Immediately after the incubation the medium was removed quickly, the wells were washed twice with DPBS (Invitrogen), and then the cells were lysed by addition of 400 μl/well radioimmunoprecipitation assay buffer (50 mM Tris-Cl, pH 7.4, 150 mM NaCl, 1% Triton X-100, 0.1% SDS and 1% sodium deoxycholate, all from Sigma) and shaken slowly for at least 1 h. From each well, 300 μl of the lysate was transferred to a scintillation vial, and the radioactivity was determined. Each experimental condition was assayed in quadruplicate in each experiment, and each experiment was performed at least three times. Data were fit to the Hill equation, and K_i values were calculated using Origin software (OriginLab Corp.). For statistical analyses, the embedded statistical tools in the Origin software were used.

Intracellular Ca^{2+} Imaging. TRPV1 expressing CHO cells were plated onto 25-mm round, glass coverslips 2 days before measurement of the intracellular Ca^{2+} ($[Ca^{2+}]_i$). The next day, the maintaining medium was switched to inducing medium that included 1 mM sodium butyrate (Sigma). On the day of measurement, cells were incubated for 1.5 h at room temperature with inducing medium containing 10 μM Fura-2 AM (Invitrogen) to permit uptake of the Fura-2. The measurements were carried out in DPBS containing 0.25 mg/ml BSA, or in DPBS without Ca^{2+} and Mg^{2+} supplemented with 10 mM EDTA and 0.25 mg/ml BSA. The fluorescence of individual cells was measured with a fluorescence imaging system (InCyt Im2; Intracellular Imaging Inc., Cincinnati, OH). During measurement, cells were alternatively illuminated at 340 and 380 nm, and the light emitted at 510 nm was collected. Data were analyzed and processed with Origin software (OriginLab Corp.).

Confocal Microscopy. CHO and CHO-rTRPV1 cells were plated onto Delta T dishes (Bioptechs, Butler, PA) 2 days before confocal microscopy experiments. On the following day, CHO cells were transfected with 2 μg/dish TRPV1-GFP plasmid as described above. Confocal microscopy experiments were performed the day after transfection. CHO-rTRPV1 cells were maintained and induced as described in the Ca^{2+} imaging section. On the day of the experiments, induced cells that were to be imaged for Golgi localization

were loaded with 0.5 μM BODIPY FL-labeled Brefeldin A dye (Invitrogen) for 30 min. Images were acquired using a confocal microscopy system (Zeiss LSM 510; Carl Zeiss Inc., Thornwood, NY) with an Axiovert 100 M microscope and a Plan Apochromat 63×/1.4 numerical aperture DIC objective. Using a multitrack configuration for sequential excitation, red and green emission was collected with a LP 560 filter and a BP 505-530 filter, respectively. For measurement of cellular uptake of CHK-884, five optical Z slices were taken every 5 min for 2.5 h, then the fluorescence intensity of the cells was measured as a function of time with Zeiss LSM 510 confocal software. Data points were fit by Levenberg-Marquardt nonlinear regression to a two-compartment uptake model using Origin software (OriginLab Corp.).

Determination of Log *P*. The octanol/water partition coefficients for 5-iodo-RTX and olvanil were determined using the LogKow software package (Syracuse Research Corporation, North Syracuse, NY), which is based on the algorithm of Meylan and Howard (Meylan and Howard, 1995). The log *P* of CHK-884 was determined by calculating the relative contribution of the tetravalent boron atom in BODIPY FL, which had previously been empirically calculated by the shake-flask method and incorporating this value into the calculations as described previously (Braun et al., 2005a).

Results

We wished to investigate the kinetics of uptake and localization of a vanilloid ligand for comparison with the kinetics of response to the ligand as determined by calcium entry and intracellular calcium levels. We therefore synthesized a fluorescent ligand CHK-884, a vanilloid that incorporates a BODIPY TR group in the vanilloid "C-region" (Fig. 1). This fluorescent capsaicin analog, which we designed based on its fluorescent characteristics and its synthetic accessibility, was correspondingly not optimal in its C-region for TRPV1 interaction and proved to be a relatively weak TRPV1 ligand. As evaluated by competition with [^{3}H]RTX for binding to rTRPV1, its K_i was 6400 ± 230 nM (mean ± S.E.M, n = 3 experiments) (Fig. 2A). Moreover, at a 30 μM ligand concentration (the maximum concentration evaluated because of concerns about solubility), CHK-884 inhibited only 70% of the [^{3}H]RTX binding. For comparison, the K_i for capsaicin under these assay conditions was 1800 ± 300 nM, indicating that CHK-884 was 3.6-fold less potent than capsaicin in the rTRPV1 binding assay.

Uptake of $^{45}Ca^{2+}$ provides a functional assay for ligand potency, and vanilloid structure activity relations with this assay often show significant differences from those determined by inhibition of [^{3}H]RTX binding (Acs et al., 1996). Using a 5-min incubation time, the half-maximally-effective concentration (EC_{50}) for CHK-884 was 2800 ± 130 nM (mean ± S.E.M., n = 9 experiments) (Fig. 2B). At longer incubation times of 15 and 30 min, the EC_{50} values were modestly more potent (1200 ± 120 and 1000 ± 140 nM, respectively; mean ± S.E.M., n = 9 experiments, $p < 0.001$ relative to 5-min incubation) (Fig. 2C). For comparison, the EC_{50} values of capsaicin under these assay conditions were 126 ± 21 and 124 ± 11 for 30 min (mean ± S.E.M., n = 3 experiments); CHK-884 was thus 22-fold less potent than capsaicin in this functional assay. For some vanilloids, BSA has been reported to influence apparent activity (Szallasi et al., 1992). Over the concentration range of 0.05 to 0.25 mg/ml, BSA did not affect the measured potency of CHK-884 (data not shown).

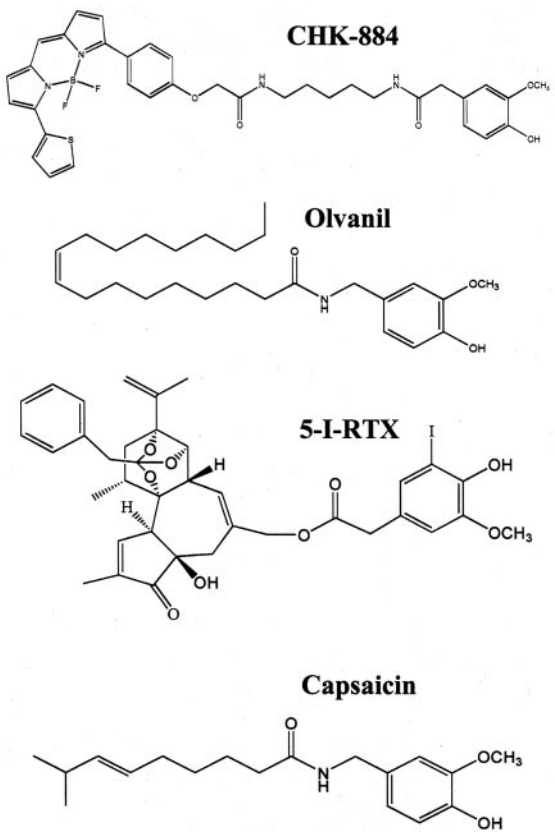

Fig. 1. Structure of vanilloids.

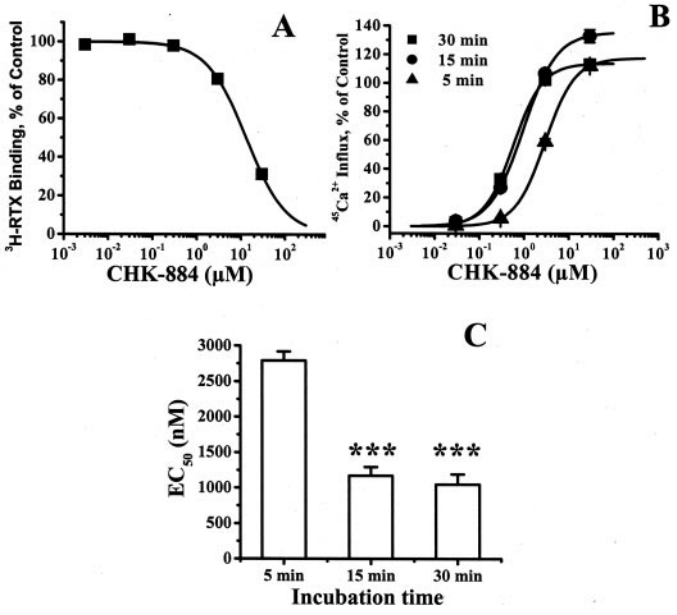

Fig. 2. Pharmacological properties of CHK-884. A, inhibition of binding of [^{3}H]RTX by CHK-884. Binding of 100 pM [^{3}H]RTX to membranes of CHO cells expressing rTRPV1 was inhibited with increasing concentrations of CHK-884 as described in methods. Results are of a representative experiment. Two additional experiments yielded similar results. (Error bars are smaller than symbols.) B, representative result of induction of $^{45}Ca^{2+}$ uptake as a function of CHK-884 concentration. Incubation was for 5 (▲), 15 (●), or 30 (■) min at 37°C. Results are expressed as the percentage of $^{45}Ca^{2+}$ uptake induced by 300 nM capsaicin. Two additional experiments yielded similar results. (Error bars are smaller than symbols.) C, EC_{50} values for induction of $^{45}Ca^{2+}$ uptake as a function of incubation time. Results are the mean and S.E.M. of nine independent experiments (***, $p < 0.001$).

Uptake of CHK-884 into cells was visualized using confocal microscopy, with the total fluorescent signal in individual cells determined as a function of time. In contrast to the very rapid uptake of capsaicin, as indicated by calcium response (Jung et al., 1999), CHK-884 penetrated only slowly. At 250 nM CHK-884, the half-time for uptake was 1800 ± 240 s, indicating that 6160 ± 310 s (mean ± S.E.M., $n = 3$ experiments) was required to reach 95% saturation under these conditions (Fig. 3). Two factors that may have contributed to this slow rate of penetration were CHK-884's large molecular size and its relatively low lipophilicity relative to that of capsaicin, as reflected by log P values of 1.38 for CHK-884 versus 4.00 for capsaicin.

Confocal microscopy also allowed the intracellular localization of CHK-884 to be determined as a function of time. We further compared the localization of CHK-884 with that of TRPV1 and with membrane markers. For comparison of the localization of CHK-884 with that of TRPV1, we transfected CHO cells with a plasmid encoding green fluorescent protein tagged rat vanilloid receptor (rTRPV1-GFP). On the day after transfection, cells were treated with 250 nM CHK-884 and visualized. For comparison of the localization of CHK-884 with that of membrane markers, cells were loaded with 0.5 μM BODIPY FL-labeled Brefeldin A dye, which marks both the endoplasmic reticulum and Golgi apparatus (Deng et al., 1995).

First, the figures clearly illustrate the slow rate of uptake of the CHK-884, as discussed above (Fig. 4). Secondly, it is striking that the fluorescent capsaicin analog localized almost exclusively to internal membranes rather than to the plasma membrane, both in control CHO cells (Fig. 4B) and in those transfected with rTRPV1-GFP (Fig. 4A). This pattern reflects the relative predominance of the internal membranes and is similar to that observed previously for phorbol esters (Braun et al., 2005a). It likewise mirrors approximately the distribution of rTRPV1-GFP, of which very little is evident at the plasma membrane, although clearly some must be present there based on the $^{45}Ca^{2+}$ measurements (Fig. 4A). Finally, the different patterns of distribution of CHK-884 over time in control cells and in cells expressing rTRPV1 should be noted. As we described previously (Olah et al., 2001), the influx of calcium triggered by the vanilloid in the presence of rTRPV1 induces re-arrangement of the intracellular membranes and of the associated rTRPV1. Because of the great excess of CHK-884 relative to rTRPV1, the contribution to the apparent localization of CHK-884 of that CHK-884 complexed to receptor would be negligible.

The slow rate of entry of CHK-884 into the cells suggested that CHK-884 should progressively activate TRPV1 with time, to the extent that this activation was not counterbalanced by TRPV1 desensitization. We therefore examined the influence of CHK-884 treatment on intracellular calcium concentration ($[Ca^{2+}]_i$) as a function of time. rTRPV1-CHO cells were incubated for 1.5 h with 10 μM Fura-2 AM in inducing medium to load the cells with the calcium indicator dye. Changes in intracellular calcium levels were then monitored in terms of the ratio of the fluorescent signal upon illumination at 340 nm and 380 nm using the InCyt calcium imaging system. In each experiment, cells were monitored for a minimum of 90 s to establish the baseline signal for $[Ca^{2+}]_i$ in DPBS with Ca^{2+}, Mg^{2+}, and 0.25 mg/ml BSA. The indicated concentration of CHK-884 was then added and the signal for $[Ca^{2+}]_i$ was monitored for a further 60 to 70 min. Separate wells of cells were used with each concentration of CHK-884. Dose-response curves (Fig. 5B) were constructed from the data points read at 3600 s at each different CHK-884 concentration for 40 to 49 individual rTRPV1-CHO cells within the microscope field (Fig. 5A). Capsaicin (300 nM) was used as a positive control. The EC_{50} of CHK-884 under these conditions was 37 ± 3 nM (mean ± S.E.M., $n = 3$ experiments). For comparison, the EC_{50} of CHK-884 determined at 5 min after addition of compound was 120 ± 10 nM (mean ± S.E.M., $n = 3$ experiments). Under the same assay conditions, the EC_{50} for capsaicin was 86.9 ± 7.7 nM at 60 min and 86.6 ± 3.7 nM (mean ± S.E.M., $n = 3$ experiments) at 5 min. The calcium imaging thus reveals that CHK-884 was more

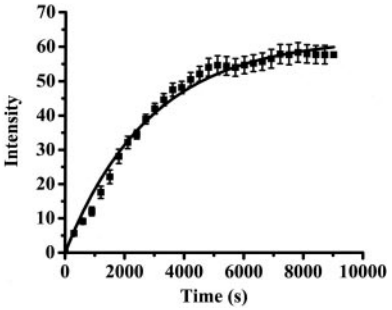

Fig. 3. Uptake of CHK-884 as a function of time. rTRPV1-CHO cells were treated with 250 nM CHK-884 and uptake visualized and quantitated by confocal microscopy as described under *Materials and Methods*. Representative result is from a single experiment. Two additional experiments with at least five cells each yielded similar results.

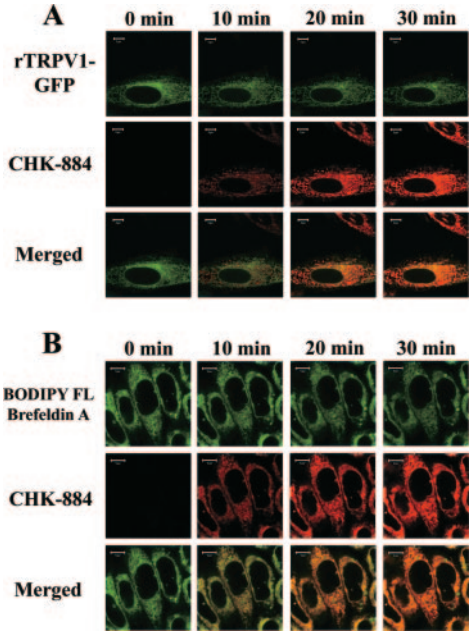

Fig. 4. Intracellular localization of CHK-884. A, CHO cells were transfected with 2 μg of rTRPV1-GFP plasmid. On the following day confocal images were taken at 1-min intervals of the rTRPV1-GFP expressing CHO cells (green) in the presence of 250 nM CHK-884 (red) (A). The images shown are representative of triplicate experiments conducted. (Bar corresponds to 5 μm.) B, rTRPV1-CHO cells were loaded with 0.5 μM BODIPY FL-labeled Brefeldin A dye (green) for 30 min, and then cells were treated with 250 nM CHK-884 (red) and visualized by confocal microscopy. (Bar corresponds to 5 μm.) The images shown are representative of triplicate experiments conducted.

potent (3.2-fold) when assayed at 60 min than at 5 min. Although this difference is less than would have been predicted (7-fold) simply from the slow rate of penetration of CHK-884, desensitization of the TRPV1 response with time would of course tend to counterbalance the apparent increase in potency with time as a result of the slow penetration.

To get a preliminary measure of whether this explanation was plausible, we treated the cells for 30 or 60 min with CHK-884 (20 or 30 nM), and then challenged with 15 or 30 nM capsaicin. The response was monitored by calcium imaging. The treatment with CHK-884 reduced the response to capsaicin relative to that seen in cells not first exposed to the CHK-884 (data not shown; single experiments under each set of conditions). Likewise, we confirmed in triplicate experiments that pretreatment (for 60 min) with capsaicin reduced the extent of stimulation of the uptake of $^{45}Ca^{2+}$ upon rechallenge with capsaicin (data not shown).

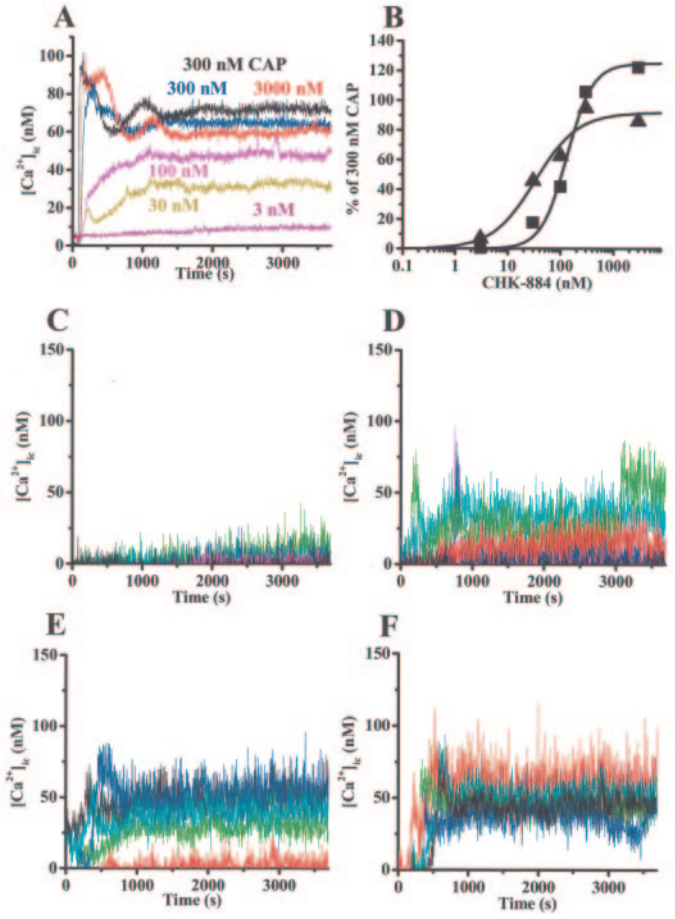

Fig. 5. Increase in $[Ca^{2+}]_i$ of rTRPV1-CHO cells in response to CHK-884. rTRPV1-CHO cells were loaded with 10 μM Fura-2 AM for 1.5 h before intracellular Ca^{2+} imaging. In every experiment, the resting $[Ca^{2+}]_i$ of 40 to 49 induced CHO-rTRPV1 cells was measured for 90 s, then CHK-884 at the indicated concentration was applied. Separate coverslips of cells were used for each time course at each CHK-884 concentration. As control 300 nM capsaicin (CAP) was used. A, time courses for the pooled data from the individual cells treated with the indicated concentrations of CHK-884. Data are from a single experiment. Two additional experiments yielded similar results. B, dose-response curves for the increase in $[Ca^{2+}]_i$ as a function of CHK-884 concentration, evaluated at 300 (■) and 3600 s (▲). Data points were determined on Fig. 5A, two additional experiments yielded similar results. C–F, for illustrative purposes, the responses of approximately six individual cells to treatment with 3 nM (C), 30 nM (D) 100 nM (E), and 300 nM (F) CHK-884 are shown. Data are from a single experiment. Two additional experiments yielded similar results.

It is noteworthy that the potency of CHK-884 was appreciably greater as measured by calcium imaging than by $^{45}Ca^{2+}$ uptake (120 versus 2800 nM, both at 5 min), whereas there was only a small difference for capsaicin (86 versus 126 nM). We do not know the basis for this difference, but we can exclude the possibility that the calcium imaging response we observe is dominated by release from intracellular stores. In the absence of external calcium, the response to thapsigargin or vanilloids that we observe in our cells is much smaller than the response to vanilloids observed under our usual assay conditions. Finally, it is noteworthy that, as measured by calcium imaging at 60 min, CHK-884 was only 2-fold less potent than capsaicin.

The InCyt imaging system permits analysis not only of the aggregate signal from the imaged cells but also tracking of the signal of the different individual cells. We have described elsewhere (Tóth et al., 2005) that the pattern of response of individual cells depends on the specific ligand as well as on its concentration. Thus, increasing doses of capsaicin cause a rapid response in most of the cells but with a graded magnitude of the response depending on the concentration of the capsaicin. For RTX, on the other hand, the typical pattern is for individual cells to respond at variable times but with a full response in each responding cell; as the concentration of RTX is increased, the average latency time before response decreases. In the case of CHK-884, we observe a different pattern. Here, we observe that at lower concentrations of CHK-884 (3 and 30 nM), the intracellular Ca^{2+} concentration in individual cells slowly increased (Fig. 5, C–D). At higher concentrations [100 nM (Fig. 5E) and 300 nM (Fig. 5F)], increasing numbers of cells responded within the first 500 s, reaching a plateau level of $[Ca^{2+}]_i$.

Olvanil. The measured slow uptake of CHK-884 motivated us to look at several other vanilloid ligands that are also candidates for showing slow uptake, although it was not possible to measure their uptake directly. The first compound was olvanil, which has been described as a potent nonpungent agonist of TRPV1. Olvanil has a calculated log *P* of 8.00, and we know that phorbol esters with a log *P* in this range enter cells slowly (Braun et al., 2005a) and only slowly induce responses of their intracellular target, protein kinase C (Wang et al., 2000; Braun et al., 2005b). In our standard $^{45}Ca^{2+}$ uptake assay with a 5-min incubation time, the EC_{50} for olvanil was 115 ± 32 nM; the EC_{50} for $^{45}Ca^{2+}$ uptake determined with a 30-min assay was only slightly lower at 81 ± 12 nM (mean ± S.E.M., $n = 3$ experiments). By calcium imaging, evaluated at 60 min, the EC_{50} of olvanil was 4.3 ± 0.6 nM (mean ± S.E.M., $n = 3$ experiments); at 5 min it was 29.5 ± 9.4 nM (mean ± S.E.M., $n = 3$ experiments) (Fig. 6, A and B). Olvanil thus seemed 7-fold more potent at the longer assay time by calcium imaging. Relative to the $^{45}Ca^{2+}$ uptake assay, the calcium imaging yielded greater potency both at early and late times, as seen for CHK-884.

Examination of the patterns of calcium influx into the cells revealed that the amplitude of response and the number of responding cells showed marked concentration dependence. At 2.5 nM olvanil, some of the cells showed slowly increasing $[Ca^{2+}]_i$; in others, the $[Ca^{2+}]_i$ rapidly increased but with different times of onset of response and then remained constant (Fig. 6C). At increasing olvanil concentrations (Fig. 6,

D–F), the predominant response was a rapid increase in $[Ca^{2+}]_i$ in individual cells with variable time of onset, where the delay before onset decreased as the concentration of olvanil increased. This latter pattern is similar to that which we described for RTX.

5-Iodo-RTX. Olvanil is an example of a highly lipophilic agonist. We selected 5-iodo-RTX as an example of a lipophilic antagonist. Its calculated log *P* is 8.03, similar to that of olvanil, and its structural similarity to the phorbol esters and related ligands of protein kinase C, for which we had previously shown slow uptake and onset of action, suggested that 5-iodo-RTX would likewise show appreciable time dependence. The K_i of 5-iodo-RTX for inhibition of [^{3}H]RTX binding was 0.61 ± 0.08 nM (mean ± S.E.M., n = 3 experiments). To determine its K_i for inhibition of $^{45}Ca^{2+}$ uptake, 5-iodo-RTX was incubated with rTRPV1-CHO cells for 0, 60, and 120 min at 37°C before addition of 50 nM capsaicin as agonist. The time of incubation with the 5-iodo-RTX had a dramatic effect on its measured potency as an antagonist (Fig. 7A). Without I-RTX preincubation, the apparent K_i was 1.42 ± 0.27 nM; after 1-h preincubation, it dropped to 21.83 ± 1.54 pM, and after 2-h preincubation, it further decreased to 3.85 ± 1.35 pM (Fig. 7B). We conclude that 5-iodo-RTX is a considerably more potent antagonist than has been recognized if the incubation time is sufficiently long. The results emphasize again that slow penetration may have an important influence on the measured potencies of vanilloids.

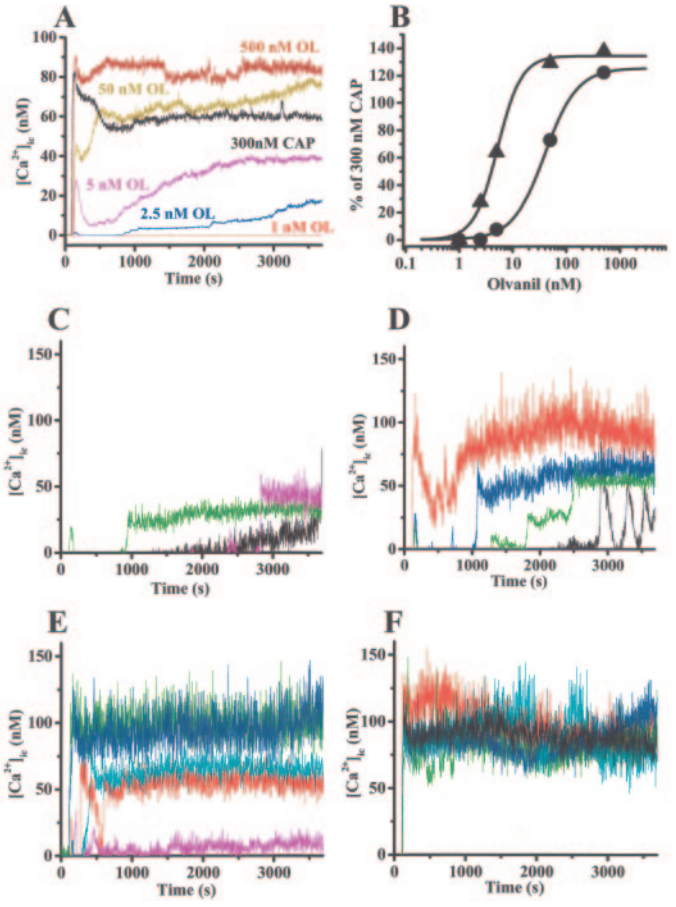

Fig. 6. Increase in $[Ca^{2+}]_i$ of rTRPV1-CHO cells in response to olvanil. rTRPV1-CHO cells were loaded with 10 μM Fura-2 AM for 1.5 h before intracellular Ca^{2+} imaging. In every experiment, the resting $[Ca^{2+}]_i$ of 40 to 49 induced CHO-rTRPV1 cells was measured for 90 s, then olvanil (OL) at the indicated concentration was applied. Separate coverslips of cells were used for each time course at each olvanil concentration. Capsaicin (CAP; 300 nM) was used as control. A, time courses for the pooled data from the individual cells treated with the indicated concentrations of olvanil. Data are from a single experiment. Two additional experiments yielded similar results. B, dose-response curves for the increase in $[Ca^{2+}]_i$ as a function of olvanil concentration, evaluated at 300 (●) and 3600 s (▲). Data points were determined in A. C–F, the responses of approximately six individual cells to treatment with 2.5 nM (C), 5 nM (D) 50 nM (E), and 500 nM (F) olvanil are shown. Data are from a single experiment. Two additional experiments yielded similar results.

Discussion

We have demonstrated in this report that the BODIPY TR labeled fluorescent capsaicin analog (CHK-884) only penetrated cells slowly, with a $t_{1/2}$ of 30 ± 4 min measured for uptake of the fluorescent ligand. This slow rate of penetration was accompanied by an increase in potency (3.2-fold) when assayed by calcium imaging at 60 min compared with 5 min. Although this increase was approximately half of what would have been predicted from the slow rate of penetration of CHK-884, it will reflect the changes in calcium handling in response to calcium influx, including the effect of desensitization. We confirmed, for example, that treatment with a limiting amount of CHK-884 reduced the response as determined by calcium imaging to subsequent challenge by a limiting amount of capsaicin. We likewise confirmed that capsaicin pretreatment caused partial desensitization to subsequent challenge with capsaicin as determined by $^{45}Ca^{2+}$ uptake.

Whereas CHK-884 may have penetrated the cells slowly because of its relatively bulky size and/or its relative hydrophilicity, olvanil might be expected to penetrate slowly on account of its substantial hydrophobicity. The EC_{50} of olvanil by calcium imaging was 4.3 ± 0.6 nM for a 60-min incubation, which compares with an EC_{50} of 29.5 ± 9.4 nM mea-

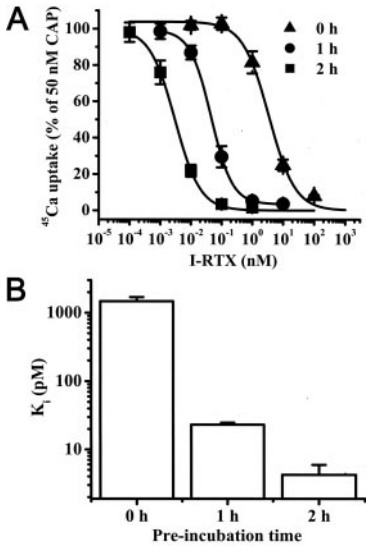

Fig. 7. Effect of preincubation time with I-RTX on TRPV1 antagonism. rTRPV1-CHO cells were preincubated with different I-RTX concentrations for 0 (▲), 60 (●), and 120 (■) min at 37°C, then antagonism of $^{45}Ca^{2+}$-uptake was determined using 50 nM capsaicin as agonist. A, inhibition curves. Data points represent the mean ± S.E.M. of four determinations in a single experiment; the inhibition curves were fitted to the Hill equation. Two additional experiments yielded similar results. B, the mean apparent K_i values as a function of preincubation time (n = 3 experiments).

sured at 5 min. These results suggest that short incubation times may significantly underestimate potency for some ligands.

A range of potencies have been reported for olvanil in various systems expressing rTRPV1, with measurements of changes in intracellular calcium. Jerman et al. (2000) reported a pEC_{50} for olvanil of 7.16 (EC_{50} = 69 nM). Phillips et al. (2004) gave a value of pEC_{50} = 6.71 (195 nM). Jerman et al. (2002) reported a pEC_{50} of 8.37 (4.3 nM). Jerman et al. (2000) stated that the kinetics for the increase in intracellular calcium in response to olvanil was similar to that of capsaicin (peak at 30 s). However, these measurements were made at a concentration of 100 nM olvanil, whereas the slow rate of penetration in our studies was evident only when limiting concentrations were used.

Olvanil is an archetype of a non pungent vanilloid agonist (Brand et al., 1987). Although the basis for its lack of pungency has not been resolved, olvanil was shown to activate TRPV1 more slowly than did capsaicin (Liu et al., 1997), and this slower activation was suggested to account for the reduced pungency (Liu et al., 1997). Likewise, it has been suggested that a slow rate of penetration, either at the cellular or tissue level, may contribute to this pharmacological profile (Wrigglesworth et al., 1996; Iida et al., 2003). It is thus particularly important that agonist assays be carried out with a sufficiently long observation time to capture the actual potency of such compounds.

A problem in the evaluation of agonists using a fixed incubation time is that response may be obscured by desensitization subsequent to the initial influx of calcium. For full antagonists, allowing sufficient time for penetration before challenge with an agonist should not be a problem. In practice, however, the existence of partial antagonists/partial agonists, sometimes with quite limited agonism, provides a complication (Wang et al., 2003).

5-Iodo-RTX is of interest as the most potent TRPV1 antagonist yet described. It also seems likely to penetrate slowly. Its predicted log *P* value is 8.03. We know that fluorescent phorbol esters with such a hydrophobicity penetrate slowly (Braun et al., 2005a) and that nonfluorescent phorbol esters with similar lipophilicity activate protein kinase C slowly (Braun et al., 2005b) and cause slow membrane translocation of protein kinase C (a measure of its interaction) (Wang et al., 2000). Furthermore, [^{3}H]RTX has slow kinetics of binding and release (Acs and Blumberg, 1994), suggesting that 5-iodo-RTX might behave similarly even after it has penetrated.

Wahl et al. (2001) initially reported that 5-iodo-RTX reversibly bound to TRPV1 with a K_i of 5.8 nM, but with slow association and dissociation times. It inhibited currents in rTRPV1-injected oocytes when coapplied with capsaicin with an IC_{50} of 3.8 nM, but the inhibition was neither reversible nor competitive over the time scale of these experiments. Likewise, using coapplication of 5-iodo-RTX and capsaicin and current measurements by patch clamping, Seabrook et al., 2002 reported an IC_{50} of 0.7 nM. By extending the preincubation time to 2 h to permit both penetration and TRPV1 equilibration at the very low levels of ligand that proved to be active, we found that 5-iodo-RTX, already an impressive antagonist based on the initial reports, seemed even more impressive, with a potency that was 1 to 2 orders of magnitude greater.

It should be emphasized that the pharmacology of 5-iodo-RTX is highly complex. One recent example is the report by Shimizu et al. (2005) that 5-iodo-RTX behaved as a partial agonist at high concentrations, whereas it acted as a full antagonist at lower concentrations (behavior that we have not observed in our control agonist or antagonist $^{45}Ca^{2+}$ uptake experiments with rat TRPV1 expressing CHO cells). Despite such mechanistic complications, the conclusion remains that short incubation times greatly underestimate the potency of 5-iodo-RTX evaluated at longer times.

Resiniferatoxin has provided a challenge to medicinal chemists, in that it demonstrated that it was possible for an agonist to be 3 to 4 orders of magnitude more potent than capsaicin. 5-Iodo-RTX likewise demonstrates that it is possible with antagonists to achieve extreme potency, orders of magnitude more potent than, for example, *N*-(4-tertiarybutylphenyl)-4-(3-chloropyridin-2-yl)tetrahydropyrazine-1(2*H*)-carboxamide (Valenzano et al., 2003).

The past few years have seen dramatic progress in the advancement of TRPV1 as a therapeutic target, with the development of potent agonists and with the identification of an impressive array of potent, structurally distinct antagonists. As development of these initial leads moves forward, the complexity of TRPV1 potentially provides opportunities beyond further enhanced potency or bioavailability. One such potential opportunity is the complex cellular localization of TRPV1, coupled with barriers to access and time dependent regulation. We demonstrate here directly that the vanilloid CHK-884 only slowly enters cells and demonstrate for two other vanilloids of biological interest that their behavior is significantly different if assessed over longer time intervals. The recognition of slow onset of action is not new. We previously had demonstrated the consequences of high lipophilicity for kinetics of inhibition of [^{3}H]RTX binding (Szallasi et al., 1991) and demonstrated in that study that the loss of pungency of capsaicin analogs of increasing lipophilicity did not reflect a loss of intrinsic receptor potency. The dissociation between pungency and intrinsic potency of *O*-ethylamine substituted vanilloids has likewise been suggested to reflect its rate of membrane penetration (Wrigglesworth et al., 1996). Nonetheless, screening for structural leads often relies on short-term incubations. Better understanding of which conditions for cellular screening have the most predictive power for the more involved animal testing might be desirable.

References

Acs G and Blumberg PM (1994) Comparison of [^{3}H]resiniferatoxin binding to spinal cord and dorsal root ganglia of newborn and adult rats. *Life Sci* **54:**1875–1882.

Acs G, Lee J, Marquez VE, and Blumberg PM (1996) Distinct structure-activity relations for stimulation of ^{45}Ca uptake and for high affinity binding in cultured rat dorsal root ganglion neurons and dorsal root ganglion membranes. *Brain Res Mol Brain Res* **35:**173–182.

Brand L, Berman E, Schwen R, Loomans M, Janusz J, Bohne R, Maddin C, Gardner J, Lahann T, Farmer R, et al. (1987) NE-19550: a novel, orally active anti-inflammatory analgesic. *Drugs Exp Clin Res* **13:**259–265.

Braun DC, Cao Y, Wang S, Garfield SH, Min Hur G, and Blumberg PM (2005a) Role of phorbol ester localization in determining protein kinase C or RasGRP3 translocation: real-time analysis using fluorescent ligands and proteins. *Mol Cancer Ther* **4:**141–150.

Braun DC, Garfield SH, and Blumberg PM (2005b) Analysis by FRET of the interaction between ligands and protein kinase C delta in the intact cell. *J Biol Chem* **280:**8164–8171.

Caterina MJ, Schumacher MA, Tominaga M, Rosen TA, Levine JD, and Julius D (1997) The capsaicin receptor: a heat-activated ion channel in the pain pathway. *Nature (Lond)* **389:**816–824.

Chou MZ, Mtui T, Gao Y-D, Kohler M, and Middleton RE (2004) Resiniferatoxin binds to the capsaicin receptor (TRPV1) near the extracellular side of the S4 transmembrane domain. *Biochemistry* **43:**2501–2511.

Deng Y, Bennink JR, Kang HC, Haugland RP, and Yewdell JW (1995) Fluorescent conjugates of brefeldin A selectively stain the endoplasmic reticulum and Golgi complex of living cells. *J Histochem Cytochem* **43:**907–915.

De Petrocellis L, Bisogno T, Maccarrone M, Davis JB, Finazzi-Agro A, and Di Marzo V (2001) The activity of anandamide at vanilloid VR1 receptors requires facilitated transport across the cell membrane and is limited by intracellular metabolism. *J Biol Chem* **276:**12856–12863.

Eun SY, Jung SJ, Park YK, Kwak J, Kim SJ, and Kim J (2001) Effects of capsaicin on Ca^{2+} release from the intracellular Ca^{2+} stores in the dorsal root ganglion cells of adult rats. *Biochem Biophys Res Commun* **285:**1114–1120.

Gavva NR, Klionsky L, Qu Y, Shi L, Tamir R, Edenson S, Zhang TJ, Viswanadhan VN, Tóth A, Pearce LV, et al. (2004) Molecular determinants of vanilloid sensitivity in TRPV1. *J Biol Chem* **279:**20283–20295.

Hwang SW, Cho H, Kwak J, Lee SY, Kang CJ, Jung J, Cho S, Min KH, Suh YG, Kim D, et al. (2000) Direct activation of capsaicin receptors by products of lipoxygenases: endogenous capsaicin-like substances. *Proc Natl Acad Sci USA* **97:**6155–6160.

Iida T, Moriyama T, Kobata K, Morita A, Murayama N, Hashizume S, Fushiki T, Yazawa S, Watanabe T, and Tominaga M (2003) TRPV1 activation and induction of nociceptive response by a non-pungent capsaicin-like compound, capsiate. *Neuropharmacology* **44:**958–967.

Jerman JC, Brough SJ, Prinjha R, Harries MH, Davis JB, and Smart D (2000) Characterization using FLIPR of rat vanilloid receptor (rVR1) pharmacology. *Br J Pharmacol* **130:**916–922.

Jerman JC, Gray J, Brough SJ, Ooi L, Owen D, Davis JB, and Smart D (2002) Comparison of effects of anandamide at recombinant and endogenous rat vanilloid receptors. *Br J Anaesth* **89:**882–887.

Jordt SE and Julius D (2002) Molecular basis for species-specific sensitivity to 'hot' chili peppers. *Cell* **108:**421–430.

Jung J, Hwang SW, Kwak J, Lee SY, Kang CJ, Kim WB, Kim D, and Oh U (1999) Capsaicin binds to the intracellular domain of the capsaicin-activated ion channel. *J Neurosci* **19:**529–538.

Liu L, Lo Y-C, Chen I-J, and Simon SA (1997) The responses of rat trigeminal ganglion neurons to capsaicin and two nonpungent vanilloid receptor agonists, olvanil and glyceryl nonamide. *J Neurosci* **17:**4101–4111.

Marshall IC, Owen DE, Cripps TV, Davis JB, McNulty S, and Smart D (2003) Activation of vanilloid receptor 1 by resiniferatoxin mobilizes calcium from inositol 1,4,5-trisphosphate-sensitive stores. *Br J Pharmacol* **138:**172–176.

Meylan WM and Howard PH (1995) Atom/fragment contribution method for estimating octanol-water partition coefficients. *J Pharm Sci* **84:**83–92.

Morice AH and Geppetti P (2004) Cough. 5: The type 1 vanilloid receptor: a sensory receptor for cough. *Thorax* **59:**257–258.

Olah Z, Szabo T, Karai L, Hough C, Fields RD, Caudle RM, Blumberg PM, and Iadarola MJ (2001) Ligand-induced dynamic membrane changes and cell deletion conferred by vanilloid receptor 1. *J Biol Chem* **276:**11021–11030.

Phillips E, Reeve A, Bevan S, and McIntyre P (2004) Identification of species-specific determinants of the action of the antagonist capsazepine and the agonist PPAHV on TRPV1. *J Biol Chem* **279:**17165–17172.

Rami HK, Thompson M, Wyman P, Jerman JC, Egerton J, Brough S, Stevens AJ, Randall AD, Smart D, Gunthorpe MJ, et al. (2004) Discovery of small molecule antagonists of TRPV1. *Bioorg Med Chem Lett* **14:**3631–3634.

Robbins W (2000) Clinical applications of capsaicinoids. *Clin J Pain* **16:**S86–S89.

Seabrook GR, Sutton KG, Jarolimek W, Hollingworth GJ, Teague S, Webb J, Clark N, Boyce S, Kerby J, Ali Z, et al. (2002) Functional properties of the high-affinity TRPV1 (VR1) vanilloid receptor antagonist (4-hydroxy-5-iodo-3-methoxyphenylacetate ester) iodo-resiniferatoxin. *J Pharmacol Exp Ther* **303:**1052–1060.

Shimizu I, Iida T, Horiuchi N, and Caterina MJ (2005) 5-Iodoresiniferatoxin evokes hypothermia in mice and is a partial transient receptor potential vanilloid 1 agonist in vitro. *J Pharmacol Exp Ther* **314:**1378–1385.

Szallasi A and Blumberg PM (1989) Resiniferatoxin, a phorbol-related diterpene, acts as an ultrapotent analog of capsaicin, the irritant constituent in red pepper. *Neuroscience* **30:**515–520.

Szallasi A, Szolcsanyi J, Szallasi Z, and Blumberg PM (1991) Inhibition of [^{3}H]resiniferatoxin binding to rat dorsal root ganglion membranes as a novel approach in evaluating compounds with capsaicin-like activity. *Naunyn-Schmiedeberg's Arch Pharmacol* **344:**551–556.

Szallasi A, Lewin NE, and Blumberg PM (1992) Identification of alpha-1-acid glycoprotein (orosomucoid) as a major vanilloid binding protein in serum. *J Pharmacol Exp Ther* **262:**883–888.

Tóth A, Wang Y, Kedei N, Tran R, Pearce LV, Kang SU, Jin MK, Choi HK, Lee J, and Blumberg PM (2005) Different vanilloid agonists cause different patterns of calcium response in CHO cells heterologously expressing rat TRPV1. *Life Sci* **76:**2921–2932.

Valenzano KJ, Grant ER, Wu G, Hachicha M, Schmid L, Tafesse L, Sun Q, Rotshteyn Y, Francis J, Limberis J, et al. (2003) *N*-(4-Tertiarybutylphenyl)-4-(3-chloropyridin-2-yl)tetrahydropyrazine-1(2*H*)-carboxamide (BCTC), a novel, orally effective vanilloid receptor 1 antagonist with analgesic properties: I. In vitro characterization and pharmacokinetic properties. *J Pharmacol Exp Ther* **306:**377–386.

Vyklicky L, Lyfenko A, Kuffler DP, and Vlachova V (2003) Vanilloid receptor TRPV1 is not activated by vanilloids applied intracellularly. *Neuroreport* **14:**1061–1065.

Wahl P, Foged C, Tullin S, and Thomsen C (2001) Iodo-resiniferatoxin, a new potent vanilloid receptor antagonist. *Mol Pharmacol* **59:**9–15.

Wang QJ, Fang TW, Fenick D, Garfield S, Bienfait B, Marquez VE, and Blumberg PM (2000) The lipophilicity of phorbol esters as a critical factor in determining the pattern of translocation of protein kinase C delta fused to green fluorescent protein. *J Biol Chem* **275:**12136–12146.

Wang Y, Tóth A, Tran R, Szabo T, Welter JD, Blumberg PM, Lee J, Kang S-U, Lim J-O, and Lee J (2003) High-affinity partial agonists of the vanilloid receptor. *Mol Pharmacol* **64:**325–333.

Wrigglesworth R, Walpole CSJ, Bevan S, Campbell EA, Dray A, Hughes GA, James I, Masdin KJ, and Winter J (1996) Analogues of capsaicin with agonist activity as novel analgesic agents: Structure-activity studies. 4. Potent, orally active analgesics. *J Med Chem* **39:**4942–4951.

Zygmunt PM, Petersson J, Andersson DA, Chuang H, Sorgard M, Di Marzo V, Julius D, and Hogestatt ED (1999) Vanilloid receptors on sensory nerves mediate the vasodilator action of anandamide. *Nature (Lond)* **400:**452–457.

Address correspondence to: Peter M. Blumberg, Molecular Mechanism of Tumor Promotion, Laboratory of Cellular Carcinogenesis and Tumor Promotion, National Cancer Institute, National Institutes of Health, Bldg. 37, Room 4048, 37 Convent Drive, MSC 4255, Bethesda, MD 20892-4255. E-mail: blumberp@dc37a.nci.nih.gov